

A Waveguide for Bose-Einstein Condensates

K. Bongs, S. Burger, S. Dettmer, D. Hellweg, J. Arlt, W. Ertmer, and K. Sengstock
Institut für Quantenoptik, Universität Hannover, Welfengarten 1, 30167 Hannover, Germany
 (November 6, 2018)

We report on the creation of Bose-Einstein condensates of ^{87}Rb in a specially designed hybrid, dipole and magnetic trap. This trap naturally allows the coherent transfer of matter waves into a pure dipole potential waveguide based on a doughnut beam. Specifically, we present studies of the coherence of the ensemble in the hybrid trap and during the evolution in the waveguide by means of an autocorrelation interferometer scheme. By monitoring the expansion of the ensemble in the waveguide we observe a mean field dominated acceleration on a much longer time scale than in the free 3D expansion. Both the autocorrelation interference and the pure expansion measurements are in excellent agreement with theoretical predictions of the ensemble dynamics.

03.75.Fi, 03.75.Dg, 32.80.Pj, 42.50.Vk

The recent realization of Bose-Einstein condensation (BEC) in dilute atomic gases [1] has stimulated extensive studies on degenerate quantum gases. While most of the experimental work so far has concentrated on 3D systems, there is growing interest in systems with lower dimensionality leading to fundamentally different phenomena. The specific properties of 1D quantum gases were recently studied theoretically and discussed controversially, e.g., the existence of a pure condensate or a quasi condensate in a weakly trapped 1D system [2,3], the connection to the concept of a Luttinger liquid [4], and the behaviour of density and phase fluctuations [3]. The transfer of a Bose-Einstein condensate into a 1D system as discussed here can thus provide important information, e.g., about the coherence properties associated with the development of phase fluctuations [3]. A wealth of new phenomena is also expected to occur in 1D collisional physics which may be studied in the expansion of a dense ensemble transferred to a 1D or quasi 1D waveguide. Waveguides with high transverse frequencies provide a tool for the experimental realization of famous theoretical models such as a 1D gas of impenetrable bosons, the so called Tonks gas [5,6].

In this letter we report on the first experimental realization of the transfer of BECs into a quasi 1D waveguide created by a blue detuned hollow laser beam. To transfer the atoms coherently we have developed a new type of hybrid trap (Fig.1). This combined dipole and magnetic (DM) trap consists of a waveguide added to the 3D potential of a Ioffe type magnetic trap. It allows for a natural connection between the magnetic trap and a pure 1D waveguide geometry created by a Laguerre-Gaussian (TEM_{01}^*) laser beam. In our scheme, we directly obtain

BEC by rf evaporation in the DM-trap. By subsequently ramping down the magnetic trapping field of the DM-trap, the BEC is transferred into the pure dipole potential waveguide and its dynamics is observed. In particular the phase-coherence of the ensemble at the different stages of this process is investigated with a Bragg interferometer scheme. As a result we find a phase-coherent and mean field dominated acceleration in the waveguide on a time scale of 20 ms, much longer than the mean field release time in the usual 3D expansion of a condensate.

As a class of waveguides, dipole potentials formed by blue detuned hollow laser beams are well suited for gaining insight into different radial confinement regimes. By changing the beam parameters they can be tuned from systems with a radial energy level spacing smaller than the mean field energy of the ensemble to 1D Tonks gas systems with strong radial confinement.

Dipole potentials have previously been used to manipulate BECs. The creation of BECs in a red detuned dipole and magnetic trap [7] and studies of spinor condensates in a 3D red detuned dipole trap [8] as well as the transfer of a BEC into an optical lattice [9] were recently reported. Note however that a focused red detuned laser beam creates a 3D trapping potential whereas the blue detuned hollow TEM_{01}^* laser mode discussed here represents an open 1D waveguide.

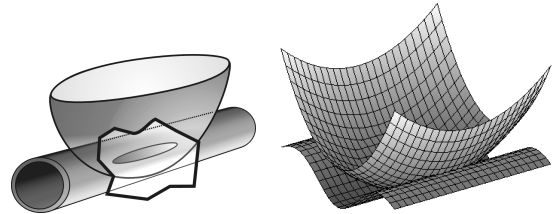


FIG. 1. Outline of the DM-trap (a) Schematic view of the potential configuration. (b) Magnetic and dipole potential in the case of matched radial oscillation frequencies.

The radially symmetric intensity distribution, $I(r)$, of a TEM_{01}^* mode is given by

$$I(r) = \frac{4Pr^2}{\pi r_0^4} \cdot e^{-2\frac{r^2}{r_0^2}}, \quad (1)$$

where P and r_0 are the laser power and the beam waist, respectively. With a power of $P = 1 \text{ W}$ at 532 nm and

a beam waist of $r_0 \approx 10 \mu\text{m}$, a dipole potential at the focal plane with a maximum value of $\sim 120 \mu\text{K} \cdot k_B$ and a transverse oscillation frequency of $\sim 6 \text{ kHz}$ for ^{87}Rb atoms can be realized. Since the atoms are guided in the low intensity region of the light field, light scattering which leads to decoherence is suppressed for atoms in the transverse ground state by more than three orders of magnitude in comparison with the scattering rate in the intensity maximum. For our measurements we adjusted the laser parameters such that the mean radial oscillation frequency of $415 \pm 10 \text{ Hz}$ matches the radial confinement of the magnetic trap with an oscillation frequency of $400 \pm 10 \text{ Hz}$. The waveguide was superimposed on the long axis of the magnetic potential (Fig.1) resulting in a DM-trap with a total radial oscillation frequency of $576 \pm 14 \text{ Hz}$ and an axial oscillation frequency of 14 Hz , solely due to the magnetic potential. Bose-Einstein condensation in the DM-trap was obtained as follows: Approximately 10^9 ^{87}Rb atoms were collected in a MOT. After their transfer to a cloverleaf magnetic trap, the atoms were cooled to a point just above the critical temperature ($T \approx 1.5T_c$) by rf induced evaporation. Then the light intensity of the waveguide potential was slowly ramped up within $\approx 15 \text{ ms}$, transferring the ensemble into the DM-trap. Subsequently a final rf evaporation ramp was applied, cooling the ensemble below T_c and thus creating a Bose-Einstein condensate of up to 2×10^5 ^{87}Rb atoms in the DM-trap. Note that the DM-trap still allows rf evaporation of atoms via the waveguide axis. We observe a lifetime of the BEC in the DM-trap on the order of one second which is comparable to the BEC lifetime observed in our pure magnetic trap. To confirm the onset of BEC we observe the sudden increase of optical density of the sample and its anisotropic expansion in a time-of-flight measurement as shown in Fig.2(a).

To investigate the phase-coherence of the ensemble in the DM-trap we use a simple two beamsplitter interferometer scheme. We also use this coherence detector to study the phase-coherence of the ensemble after transfer into the waveguide as discussed later.

The interferometer consists of only two $\frac{\pi}{2}$ Bragg pulses separated by a time t_B , applied after switching off the trapping potentials as indicated in Fig.2(b). The beamsplitters are realized by $\frac{\pi}{2}$ Bragg pulses [10,11] of counterpropagating laser beams aligned parallel to the axis of the waveguide, which split an incoming wavepacket into a coherent superposition of two wavepackets with velocities differing by $2\hbar k/m = 11.7 \text{ mm/s}$. The two laser frequencies are detuned by $\approx 6 \text{ GHz}$ from the ^{87}Rb -line at 780 nm with a fixed frequency difference set to match the Bragg condition. The two wavepackets created by the first $\frac{\pi}{2}$ -pulse separate in space during the free evolution time t_B by an amount $\Delta x = \frac{2\hbar k}{m} t_B$. The second $\frac{\pi}{2}$ -pulse then recombines the partially overlapping clouds in both exit ports of the interferometer, which again dif-

fer in momentum by $2\hbar k$. The displacement leads to interference fringes in both exit ports due to the additional phase distribution caused by the expansion of the condensate, similar to the autocorrelation measurements in the $\frac{\pi}{2} - \pi - \frac{\pi}{2}$ geometry of [13].

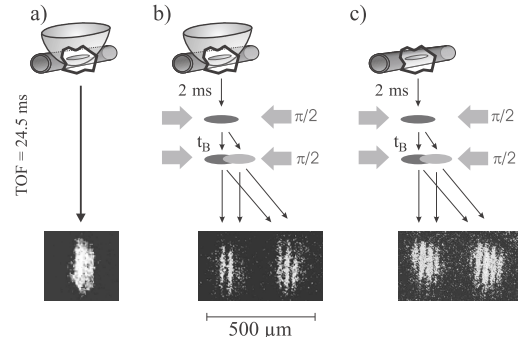


FIG. 2. a) Absorption image of an atomic cloud after 24.5 ms of time-of-flight for a BEC created in the DM-trap. b) Autocorrelation interferometer scheme and absorption image of the interference fringes for $t_B = 3 \text{ ms}$ and a total time-of-flight of 24.5 ms for an ensemble released from the DM-trap. (c) Same as (b) for $t_B = 1 \text{ ms}$ and an ensemble stored in the waveguide for an evolution time of 6 ms.

The observed spacing of the interference fringes can be understood as follows: The condensate expands mainly due to the conversion of mean field energy into kinetic energy. Since the mean field energy, U_{mf} , is proportional to the parabolic density distribution, the local acceleration $\dot{v} \propto \nabla U_{mf}$ depends linearly on position. As a consequence the ensemble keeps a parabolic density distribution during expansion while acquiring a velocity field which linearly increases with position, $v(x) = \alpha(t)x$. The velocity gradient is given by $\alpha(t) = \dot{\lambda}(t)/\lambda(t)$ with the scaling parameter $\lambda(t)$ defined in [12] indicating the size of the condensate relative to its size in the trap. The local velocity difference between the two overlapping clouds thus does not depend on position but only on the displacement and on time $\Delta v = \alpha(t)\Delta x$. The observed interference pattern therefore corresponds to the interference of two plane matter waves with a relative velocity Δv . The corresponding fringe spacing $d = \frac{h}{m\Delta v}$ can be used to deduce the velocity gradient of the ensemble

$$\alpha(t) = \frac{h}{md\Delta x}. \quad (2)$$

Note that the above discussion assumes that all mean field energy is converted to kinetic energy before the interferometer sequence. In our experiment the time-of-flight prior to the first interferometer pulse is chosen to be 2 ms in which more than 95% of the mean field energy is converted into kinetic energy.

We now turn to our measurements of phase-coherence for 3D ensembles in the DM-trap and during expansion in the quasi 1D waveguide. We obtained the interference pattern of the BEC produced in the DM-trap by

taking absorption images of the density distribution after the interferometer sequence and a total time of flight of 24.5 ms (Fig.2(b)). The time between the pulses was varied from $t_B = 1$ to 4ms resulting in a displacement of the interfering clouds of $\Delta x = 12$ to $48 \mu\text{m}$. The largest displacements roughly correspond to half the condensate size of $\approx 100 \mu\text{m}$. For all these displacements high contrast, equally spaced interference fringes were observed, demonstrating both, the coherence of the ensemble on these length scales and the validity of the above model for the 3D BECs in the DM-trap.

In a further set of experiments, the transfer of the Bose-Einstein condensed ensemble to the waveguide and the subsequent evolution of the atomic ensemble inside the waveguide were investigated.

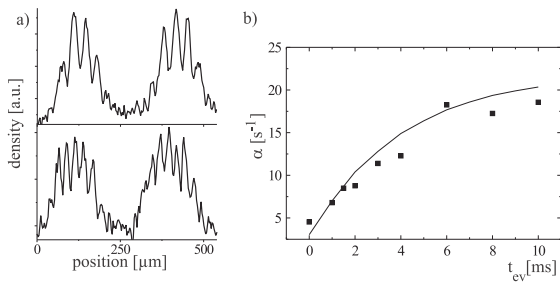


FIG. 3. (a) Interference signals from guided ensembles for evolution times of 4 ms (top) and 6 ms (bottom) in the waveguide. (b) Velocity gradient versus guiding time deduced from measurements of the fringe spacing (dots) in comparison to the numerical calculation (solid line).

Again, in a series of measurements the $\frac{\pi}{2} - \frac{\pi}{2}$ pulse interferometer scheme was now applied to an ensemble transferred from the DM-trap into the waveguide for different evolution times t_{ev} in the waveguide. For this purpose the natural connection of the DM-trap to the waveguide was demonstrated by adiabatically lowering the magnetic field, thus releasing the ensemble into the waveguide. Figure 2(c) shows an example of the resulting interference fringes. Figure 3(a) shows examples of cross sections through the interference signals. For these measurements the time between the Bragg pulses was set to 1ms, resulting in a displacement of the wavepackets of $\approx 12 \mu\text{m}$. For the first time, these interference signals clearly document the axial phase-coherence of an ensemble after the transfer of a BEC into a quasi 1D waveguide and an additional evolution time. As another important result, the equal spacing of the interference fringes confirms the linear velocity distribution predicted by the model given above (Eqn.2) for the 1D expansion in the waveguide.

The decrease of fringe spacing for increased evolution times in the waveguide demonstrates an increasing velocity spread of the wavepacket as mean field energy is converted into kinetic energy within the waveguide. We observe a decrease in fringe spacing with time even for

evolution times of 10 ms in the waveguide, i.e., the atoms are still accelerated by the mean field energy. These measurements clearly show that the conversion of mean field energy into kinetic energy is more than one order of magnitude slower than in 3D due to the reduced dimensionality inside the waveguide.

From the regular fringe spacing we deduced the spatial velocity gradient of the ensemble for different evolution times. Fig.3(b) compares this data to the result of a numerical calculation of the parameter $\alpha(t)$ according to [12]. Note that the calculation does not include any free parameters, nor depends on the particle number. The good agreement clearly demonstrates the consistency of the ensemble dynamics with a mean field dominated and phase coherent expansion inside the waveguide and the applicability of the scaling laws to the quasi 1D regime.

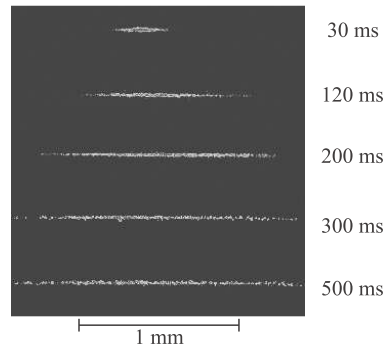


FIG. 4. Atoms from a BEC loaded to a doughnut waveguide with different evolution times inside the waveguide.

The above interferometer scheme is well suited to study the axial expansion of the ensemble inside the waveguide within the first ten milliseconds. For longer guiding times, when the ensemble density is significantly reduced we have directly studied the expansion by absorption imaging without an additional time-of-flight. Figure 4 shows examples for these measurements for evolution times up to 500 ms. On time scales above 40 ms the conversion of mean field energy into kinetic energy is nearly complete and the ensemble is expected to expand with constant velocity keeping its parabolic density distribution. We indeed found the predicted parabolic density distribution confirmed for evolution times up to 150 ms from cross sections through images as shown in Fig.4. These measurements are limited only by our field of view as no reliable fits to the data can be obtained as soon as the imaged length of the ensemble corresponds to the size of our CCD array.

An estimate of the maximum velocity at the edge of the cloud after an expansion in the waveguide can be obtained as follows: After long expansion times in the waveguide the ensemble width is much larger than its initial width. In this limit the maximum velocity at the edge of the cloud can be calculated from simple kinematics and is given by

$$v_{max} = \sqrt{\frac{10E_{kin}}{m}} \quad (3)$$

where E_{kin} is the kinetic energy per particle. If all internal energy is converted in kinetic energy, E_{kin} can be replaced by the initial internal energy E_{int} . The internal energy per particle in the Thomas-Fermi limit is well known [14] and is given by $E_{int} = 0.46k_B N^{2/5}$ nK for our experimental parameters. For $N=5 \times 10^4$ atoms we find $v_{max} = 5.8$ mm/s in good agreement with the velocity deduced from our experimental data $v_{max} = 5.9$ mm/s. This again confirms the mean field dominated expansion of the cloud in the waveguide.

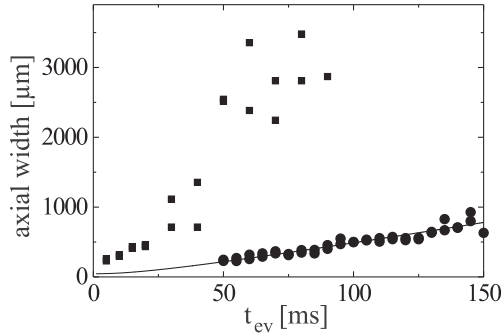


FIG. 5. Longitudinal expansion of BECs loaded into the waveguide. Squares show the Gaussian half-width of ensembles transferred from the magnetic trap. Circles represent the Thomas-Fermi half-width of ensembles adiabatically transferred from the DM-trap and the solid line corresponds to a theoretical prediction for adiabatic loading conditions with $N = 5 \times 10^4$ atoms.

Finally, we have compared different loading mechanisms of the waveguide. Figure 5 shows a comparison of the expansion of atomic clouds loaded from the DM-trap to the expansion of clouds loaded directly from a BEC created in the cloverleaf magnetic trap. The latter was done by instantly switching on the doughnut beam and switching off the magnetic trap in $200\mu s$. For direct loading from the magnetic trap, the system expands to several millimeters in length within ≈ 100 ms, which indicates the non-adiabaticity of the direct transfer process. In contrast, the cloud's expansion for loading from a BEC first created in the DM-trap shows excellent agreement with the theoretical prediction [12] of mean field dominated expansion (solid line in Fig. 5). In this case the atomic density distribution spreads out over an axial region of ≈ 1 mm within 150 ms, and the cigar-shaped BEC transforms to a straight hair of quantum gas.

In conclusion we have presented three important results, paving the way to study 1D quantum gases. First, we have observed Bose-Einstein condensation of an ensemble of ^{87}Rb atoms in a hybrid trap realized by the combined potential of a Ioffe type magnetic trap and a

blue detuned dipole waveguide potential. Second, the coherence of the ensemble in the trap and in the waveguide was measured with a simple autocorrelation interferometer scheme. Third, we investigated the transfer process of Bose-Einstein condensates into a blue detuned dipole waveguide and studied the subsequent evolution of the ensemble in a quasi 1D waveguide. In these experiments we demonstrated that a fully coherent transfer is possible by our scheme and observed a mean field dominated expansion of the ensemble for adiabatic loading conditions.

These investigations open a path for future studies of the different regimes of 1D quantum gases. The realization of a Tonks gas of impenetrable Bosons seems feasible in our geometry. After loading the dipole waveguide potential can be increased adiabatically to reach the 1D regime in which transverse degrees of freedom are fully frozen out ($\omega_r \approx 10$ kHz). As additional magnetic fields can be superimposed on the dipole potential, the scattering length a can be tuned using Feshbach resonances to achieve a suitable value for the Tonks gas regime. Also, e.g. spinor condensates [8] and dark solitons [15,16] can be investigated in 1D waveguide geometries. The waveguide can easily be closed by additional light field mirrors [17] or a superimposed weak longitudinal trapping potential. This opens opportunities for a first realization of a guided matter wave interferometer.

This work is supported by SFB 407 of the *Deutsche Forschungsgemeinschaft*.

-
- [1] M. J. Anderson, J. R. Ensher, M. R. Matthews, C. E. Wieman, and E. A. Cornell, *Science* **269**, 198 (1995); K. B. Davis, M.-O. Mewes, M. R. Andrews, N. J. van Druten, D. S. Durfee, D. M. Kurn, and W. Ketterle, *Phys. Rev. Lett.* **75**, 3969 (1995); C. C. Bradley, C. A. Sackett, and R. G. Hulet, *Phys. Rev. Lett.* **78**, 985 (1997); D. Fried et al., *Phys. Rev. Lett.* **81**, 3811 (1998)
 - [2] N. van Druten and W. Ketterle, *Phys. Rev. Lett.* **79**, 549 (1997)
 - [3] D. Petrov, G. V. Shlyapnikov and J. Walraven, *cond-mat/0006339* and references therein
 - [4] H. Monien, M. Linn and N. Elstner, *Phys. Rev. A* **58**, R3395 (1998)
 - [5] L. Tonks, *Phys. Rev.* **50**, 955 (1936)
 - [6] M. Olshanii, *Phys. Rev. Lett.* **81**, 938 (1998)
 - [7] D. M. Stamper-Kurn et al., *Phys. Rev. Lett.* **80**, 2027 (1998)
 - [8] J. Stenger et al., *Nature* **396**, 345 (1998)
 - [9] B. Anderson and M. Kasevich, *Science* **282**, 1686 (1998)
 - [10] J. Stenger et al., *Phys. Rev. Lett.* **82**, 4569 (1999)
 - [11] E.W. Hagley et al., *Phys. Rev. Lett.* **83**, 3112 (1999)
 - [12] Y. Castin and R. Dum, *Phys. Rev. Lett.* **77**, 5315 (1996)
 - [13] J. Simsarian et al, *cond-mat/0005303*
 - [14] G. Baym and C. Pethick, *Phys. Rev. Lett.* **76**, 6 (1996)

- [15] J. Denschlag et al., Science **287**, 97 (2000)
- [16] S. Burger et al., Phys. Rev. Lett. **83**, 5198 (1999)
- [17] K. Bongs et al., Phys. Rev. Lett. **83**, 3577 (1999)